

1 Article

2 **A survey of transposon landscapes in the putative**
3 **ancient asexual ostracod *Darwinula stevensoni***

4 **Isa Schön^{1,2*}, Fernando Rodriguez^{3a§}, Matthew Dunn^{3b}, Koen Martens^{1,4}, Michael**
5 **Shribak^{3c} and Irina Arkhipova^{3d}**

6 ¹ Royal Belgian Institute of Natural Sciences, OD Nature, Freshwater Biology, Vautierstraat 29, B-1000
7 Brussels, Belgium; ischoen@naturalsciences.be

8 ² University of Hasselt, Researchgroup CMK, Diepenbeek, Belgium; ORCID 0000-0001-9269-6487

9 ³ Marine Biological Laboratory, MBL Street 7, Woods Hole MA 02453, USA

10 ^a ORCID: 0000-0003-4044-8734; frodriguez@mbl.edu

11 ^b mjdunn@umass.edu

12 ^c ORCID: 0000-0002-5849-6294; mshribak@mbl.edu

13 ^d ORCID: 0000-0002-4805-1339; iarkhipova@mbl.edu

14 ⁴ University of Ghent, Dept Biology, Ghent, Belgium; ORCID: 0000-0001-8680-973X; darwinula@gmail.com;
15 ORCID: 0000-0001-8680-973X

16 * Correspondence: ischoen@naturalsciences.be

17 [§] Co-first

18 Received: date; Accepted: date; Published: date

19 **Abstract:** How asexual reproduction shapes transposable element (TE) content and
20 diversity in eukaryotic genomes remains debated. Here, we performed an initial
21 survey of TE load and diversity in the putative ancient asexual ostracod *Darwinula*
22 *stevensoni*. We examined long contiguous stretches of DNA in clones selected from
23 a genomic fosmid library, totaling about 2.5 Mb, and supplemented these data with
24 results on TE abundance and diversity from an Illumina draft genome. In contrast
25 to other TE studies in putatively ancient asexuals, which revealed relatively low TE
26 content, we found that at least 19% of fosmid DNA sequences and 26% of the
27 genome corresponded to known transposons. We observed a high diversity of
28 transposon families, including LINE, gypsy, PLE, *mariner/Tc*, *hAT*, *CMC*, *Sola2*,
29 *Ginger*, *Merlin*, *Harbinger*, MITEs and helitrons. The predominantly low levels of
30 sequence diversity indicate that many TEs are or have recently been active. No
31 correlation was found between telomeric repeats and non-LTR retrotransposons
32 present near telomeres in the fosmid data as in other taxa. We found that most TEs
33 in the fosmid data were located outside of introns and almost none were found in
34 exons. We also report an N-terminal Myb/SANT-like DNA-binding domain in site-
35 specific *R4/Dong* non-LTR retrotransposons. Although initial results on
36 transposable loads will need to be verified at a genome-wide scale with high quality
37 draft genomes, this study provides important first insights into the dynamics of
38 TEs in putative ancient asexual ostracods.

39 **Keywords:** transposable elements; retrotransposons; DNA transposons;
40 crustaceans; asexuality

Deleted: In the absence of a high-quality whole-genome draft, w...

Deleted: .1

Deleted: M

45

46 1. Introduction

47 The influence of reproductive mode on transposon content and distribution in
48 eukaryotic genomes remains a subject of debate as it seems to be shaped by several
49 evolutionary forces acting in opposite directions. Sexual reproduction is expected to
50 greatly facilitate spread of vertically transmitted transposons in populations [1], as
51 has been experimentally shown in yeast (see for example [2] or [3]).

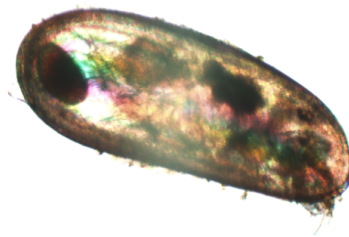
52 All asexuals originate from sexual ancestors. If they inherited transposons, the
53 absence of meiotic recombination should lead to reduced efficacy of selection and
54 accumulation of deleterious mutations [4] and transposons, at least in finite
55 populations [5,6]. Empirical evidence for these predictions comes from non-
56 recombining sex chromosomes e.g. [7] and other non-recombining parts of the
57 genome [8,9]. Such unrestrained TE proliferation should eventually drive asexual
58 lineages to extinction unless asexual hosts can keep TE copy numbers under tight
59 control [10-12], with putative ancient asexual bdelloids as the most striking example
60 [10,13,14] of having reduced numbers of vertically transmitted retrotransposons
61 while they still harbor some DNA transposons that can be horizontally transmitted.
62 In line with these predictions, sexual *Daphnia pulex* have higher loads of DNA
63 transposons [15], LTR retrotransposons [16] or more insertion polymorphisms of
64 transposons [17] than their asexual counterparts. Comparative genomic studies on
65 asexual and sexual arthropods [18], nematodes [19], evening primroses [20] and
66 green algae [21], however, did not show any significant effect of the reproductive
67 mode on transposon content and evolution. Other genomic studies reported higher
68 transposon loads in asexuals as for example for root-knot nematodes [22] or parasitic
69 wasps [23].

70 These contrasting results can partly be explained by different lineage ages [24].
71 Purging of transposons in asexuals can take a very long time, and transposons are
72 expected to accumulate if they cannot be removed [25]. Theoretical studies [26,27]
73 and an ever-increasing number of genomic studies from different host organisms
74 [28,29] suggest that additional factors besides the reproductive mode will also
75 influence transposon diversity and load, such as initial transposon load in sexual
76 ancestors, DNA methylation, population size [30], environmental fluctuations [27],
77 strengths of selection and drift [19], and molecular defense mechanisms against
78 transposable elements. DNA transposons are more frequently transmitted
79 horizontally (as in the example of insects; [31]) than retrotransposons and are
80 expected to be less affected by the reproductive mode.

81 To better understand transposon evolution, their molecular characteristics and
82 biological effects, additional *in vivo* and *in vitro* studies are thus required [28],
83 especially from non-model organisms. The continuous increase of genomic data has
84 also revealed the extent of lineage-specific transposon diversities, which further
85 increases the methodological challenges of analyzing these elements [28] and
86 provides additional motivation for studying them in a wide range of organisms.

87 The ostracod family Darwinulidae is one of the few examples of putative ancient
88 asexual animals [32-35], to which bdelloid rotifers also belong [36]. Fossil data
89 indicate that some darwinulids might have been asexual for 200 million years [37],
90 and the type species of this family that is investigated here, *Darwinula stevensoni*
91 (Figure 1), for about 25 million years [38]. There is only one study on transposable
92 elements of darwinulid ostracods describing novel LINE-like retroelements [39],
93 and long, contiguous genome assemblies from these ostracods are not yet available.

94



102 **Figure 1.** *Darwinula stevensoni*. a. A sample of multiple individuals of *Darwinula*
103 *stevensoni*. Taken by Jeroen Vendericks. b. Lateral view of the carapace of an
104 individual *Darwinula stevensoni*. This picture was taken with the polychromatic
105 polarization microscope [40] with a 4x objective lens and a DP73 camera. The total
106 length of the animals is around 800 μm . In the left corner, an embryo in the brooding
107 pouch is visible.

108
109 Here, we used long DNA sequences of *D. stevensoni* based on selected clones of
110 a genomic fosmid library, totaling around 2.5 Mb, for addressing four aims: (1) To
111 gain initial insights into TE content, diversity and activity in darwinulid ostracod
112 genomes and confirm these preliminary results with data from an Illumina draft
113 genome of *D. stevensoni*; (2) Examine possible links of TEs with telomeres; (3)
114 Compare the location of TEs to coding gene regions (CDS); (4) Assess the possible
115 impact of anciently asexual reproduction on TE landscapes of non-marine ostracods.
116 We observed a high diversity of TEs in the putative ancient asexual ostracod *D.*

Formatted: Font: Italic

117 *stevensoni*, and a high prevalence of 19-26% in the surveyed fosmid and draft genome
118 DNA sequence data. Most TEs were located outside of coding regions, had no link
119 to telomeres and showed evidence of recent activity. Our results provide first
120 indications that putative ancient asexual ostracods might not be able to efficiently
121 purge TEs from their genomes.
122

Deleted: more than

Deleted:

Deleted: 5

123 2. Materials and Methods

124 2.1. Construction, screening and sequencing of a genomic fosmid library

125 A genomic fosmid library of *D. stevensoni* was constructed at Clemson University
126 (USA) from 1000 pooled individual ostracods, sampled from the monoclonal Belgian
127 population in Hollandersgatkreek, because of the small size of these ostracods (L= c
128 0.8 mm - Figure 1a & b). Ostracods were first incubated for ten days in pure water
129 to evacuate any possible contaminants from the gut. High molecular weight DNA
130 was isolated, randomly fragmented, end-repaired, phosphorylated, and size
131 selected by pulsed-field gel electrophoresis. Size-selected fragments were ligated
132 with the linearized dephosphorylated fosmid vector pCC2FOS (NovoPro) and then
133 packaged by lambda packing extracts and plated on T1-phage resistant *E. coli*. A
134 total of 18,432 recombinant colonies were randomly picked with a Genetix Q-bot
135 robot and stored as individual clones at -80°C in 384-well microtiter plates. Fosmids
136 have an average insert size of 35 to 45 kbp, as was confirmed by randomly sampling
137 48 clones. Preliminary evaluation of *D. stevensoni* from the same Belgian population
138 with flow cytometry and DAPI staining revealed a genome size of 0.86 to 0.93 pg,
139 equaling 840 to 900 Million bp (Pacziesniak et al., unpubl. data). Karyological studies
140 have shown that *D. stevensoni* nuclei contains 22 dot-like chromosomes [41] that
141 cannot be visually grouped into homologous pairs, making it impossible to infer the
142 ploidy level of *D. stevensoni* from cytological observations.

143 To identify fosmids containing either TEs or telomeres, specific overgo probes
144 for LINE-like and mariner-like elements and telomeric repeats were developed (see
145 Table S1 for details) from published data on two LINE-like elements of *D. stevensoni*
146 [39] and unpublished data on TEs from non-marine ostracods, which had been
147 acquired with PCR walking and Sanger sequencing using the general primers of
148 [10]. Probes for telomeres were based on the universal arthropod telomeric repeat
149 (TR) with the pentameric unit TTAGG [42]. We also screened for fosmids containing
150 single-copy nuclear genes of *D. stevensoni* [43].

151 High density colony filters from the entire fosmid library were produced using
152 a Genetix Q-bot in a 4x4 double-spotted array on GE HealthCare Hybond N+
153 membranes. Labelled PCR probes were used for hybridization of high-density
154 colony filters and hits were called with Hybdecon v.01. The identity of fosmids
155 having hits for TEs, single copy nuclear genes and/or TRs was assessed. The
156 hybridization experiments with the fosmid library revealed 86 fosmids with positive
157 hits for the mariner probe, 18 for LINE-like *Daphne*, 33 for LINE-like *Syrinx* elements
158 and 40 fosmids with hits for various nuclear genes, respectively (Table S2). A set of

162 96 fosmid, of which 13 contained positive hits for chosen TEs (5 Daphne, 5 Syrinx,
163 3 mariner) and the other 83 for nuclear genes, were selected for further detailed
164 analyses. DNA was extracted and prepared for high-throughput sequencing with
165 the Ion Xpress™ plus gDNA Fragment Library preparation kit and the Ion
166 OneTouch™ 200 Template Kit v2 from Life Technologies. Individual fosmids were
167 sheared, ligated to adapters with barcodes, size selected, pooled and used for an
168 emulsion PCR. Fosmids were sequenced with the Ion PGM™ Sequencing 300 Kit on
169 the Ion Torrent PGM using the Ion 316™ chips. A total of 779M DNA basepairs and
170 2,827,903 reads were generated, with a median read lengths of 290 bp and maximum
171 lengths of 433 bp. Fosmids were demultiplexed, and quality filtering and assembly
172 conducted with CLC workbench (Qiagen; version 7.5.1) using default parameters.

173 Another 11 fosmids were selected by hybridization with probes for single
174 nuclear copy genes of potential horizontal origin (see Table S2) as part of the
175 LATTECO project at the CNRGV (INRA facility, Toulouse, France). Sequence
176 identities of the ends of positive fosmids were validated by PCR and Sanger
177 sequencing. For PacBio RS II sequencing, 2 µg of each validated fosmid was tagged
178 with PacBio tags and then pooled. The library was generated with the standard
179 Pacific Biosciences library preparation protocol for 10 kb libraries and sequenced on
180 one SMRT Cell using the P6v2 chemistry following the standard operating
181 procedures of the manufacturer at the NGI (<https://ngisweden.scilifelab.se/>).
182 Assembly of the PacBio RS II reads followed the HGAP workflow. The SMRT®
183 Analysis (v2.2.0) software suite was used for HGAP implementation. Reads were
184 first de-multiplexed and then aligned using BLASR against “*E. coli* str. K12 substr.
185 DH10B, complete genome”. Identified *E. coli* reads and low-quality reads (read
186 quality <0.80 and read length <500 bp) were removed. Filtered reads were then
187 preassembled to generate long and highly accurate sequences. To perform this step,
188 we separated the smallest and longest reads (e.g. >11 kbp) in order to correct read
189 errors by mapping the smallest to the longest reads. Obtained sequences were
190 filtered against vector sequences, and sequences were assembled into draft
191 assemblies with the Celera assembler. As the final step of the HGAP workflow,
192 “polishing” with Quiver significantly reduced remaining insertions and deletions
193 and base substitution errors, resulting in high quality assemblies of a single contig
194 per fosmid.

195 We analysed 341 contigs with a minimum length of 100bp for further analyses.

196 We also conducted BLAST searches [44] with all contigs to each other to identify
197 potentially overlapping redundant regions. The content of matching regions was
198 further checked manually. If these included identical transposons, we considered
199 them as evidence for recent transposition and kept the data. If (short) contigs fully
200 matched other contigs, they were excluded. Likewise, short overlaps at the 5′ or 3′
201 end of fosmid sequences were also excluded if they showed more than 94% overlap
202 with other contigs. In the absence of a phased reference genome, we can however
203 not be certain if overlapping contigs originate from the same chromosome or from
204 its homolog, as the allelic divergence is expected to be low, especially if the overlap
205 is relatively short. To still account for possible bias from overlapping contig ends,

Deleted: some

Deleted: most

Formatted: Highlight

Formatted: Highlight

208 we are providing ranges for contigs and fosmid total lengths and estimates of exon,
209 intron and TE content below.

210 All sequence data have been submitted to the GSS of ncbi; accession number
211 **XXXXXX**.

212 2.2. *Illumina draft genome of D. stvensoni*

213 Besides the fosmid DNA sequence data, we also analyzed a recently published
214 Illumina draft genome (European Nucleotide Archive accession number
215 PRJEB38362) of *D. stvensoni* [45] for its TE content and diversity. This draft genome
216 was assembled from DNA extractions of a single female, followed by Whole
217 Genome Amplification to provide sufficient material for the preparation of three
218 2x125bp paired-end libraries (average insert sizes of 250-300, 550 and 700bp), and
219 two mate-pair libraries (average insert sizes of 3000 and 5000bp), respectively, which
220 were sequenced on an Illumina HiSeq 3000 system. The assembly has a size of 382.1
221 Mb, an N50 of 56.4 kb, an arthropod BUSCO score of 93.7% (complete single copy
222 genes) and consists of 62,118 scaffolds [45].

223 2.3 *De novo identification of ostracod TEs*

224 We used the REPET package with default settings [46,47] for *de novo* TE
225 identification and annotation of fosmid and draft genome data in three steps:
226 detecting repeated sequences and potential TEs, clustering of these sequences, and
227 generating consensus sequences for each cluster. Consensus sequences were
228 classified following Wicker's TE classification [48] and transposons were grouped
229 by families. Repeat Masker [49] was applied for TE classification and plot building,
230 using the local fosmid and genomic libraries of *D. stvensoni* from REPET. We
231 constructed TE landscape divergence plots to evaluate the frequencies of different
232 TE families in our data set and estimate the Kimura substitution level of each TE
233 family with adjusted CpG as a measure of TE activity over time. We also translated
234 all fosmid DNA sequences and used the translated data in Censor
235 (<https://www.girinst.org/censor/>) to reveal non-multicopy TEs and to classify TEs at
236 the amino-acid level.

237 2.4. *Assessing insertion sites of TEs from fosmid data*

238 For obtaining preliminary information on the genomic location of TEs, we
239 compared hybridization signals between fosmids with positive hits for telomeres
240 and TEs. To assess if TEs were found in coding or non-coding genomic regions, we
241 used our custom TE library with Repeat Masker to identify and soft-mask all TEs.
242 The masked DNA sequence data were then used for gene predictions with Augustus
243 [50] with *Drosophila melanogaster* as species parameter. In regions being identified as
244 coding regions in the sequenced fosmids, the lengths of exons and introns were
245 calculated from the exact locations to estimate the overall frequency of exons and
246 introns in the DNA sequence data. To identify possible overlap of TEs and exons,
247 we used BEDTools v2.29.2 [51] to compare the exact exon and intron locations in

Deleted: (to be completed during review)

Formatted: Highlight

Deleted: *De novo identification of ostracod TEs*

Formatted: Font: Italic

Deleted: 45

Deleted: 46

Deleted: 47

Deleted: 48

Deleted: y

Formatted: Highlight

Commented [MOU1]: Fernando, please confirm that we only did this for the fosmid data.

Deleted: 3

Deleted: 49

Commented [MOU2]: Fernando, if you could please add the software here?

Formatted: Highlight

Deleted: 50

258 each fosmid with partial and complete TE locations as identified by Censor at the
259 amino-acid level.

260 We calculated the frequency of introns and exons, TEs and overlap with exons
261 and introns, respectively, per fosmid and visualized these as boxplots in ggplot2 [52]
262 in R [53]. For selected fosmids, we used the output files of gene predictions with
263 Augustus and TE identification by Censor to draw the positions of transcripts,
264 exons, introns and TEs with Circos [53].

265 2.5. Estimating single copy gene content in fosmid sequence data

266 To assess the representativity of selected fosmids with regard to coding
267 sequences, we conducted Benchmarking set of Universal Single-Copy Orthologs
268 (BUSCO) v3.0.2 analyses [55] of all fosmid sequence data using Arthropoda_odb9 as
269 reference database for single copy ortholog genes [56].

270 2.6. Search for remote homologies

271 To investigate the N-terminal domain in *R4/Dong* elements, we assembled a
272 dataset of 5'-complete ORFs which included phylogenetically diverse additional
273 sequences from GenBank identified by BLAST (accession numbers shown in Fig.
274 6), aligned with MUSCLE [57], extracted the N-terminal part upstream of the
275 reverse transcriptase domain, and used the multiple sequence alignment as a query
276 on the HHPred server [58] with default settings. The C-terminal extension of
277 *DsGypsy1* had no detectable homologs and was used as a standalone query. The
278 seed alignment for PF00249 (*Myb_DNA-binding*) was downloaded from PFAM
279 (<http://pfam.xfam.org/>). Structure-based alignments obtained with HHPred were
280 visualized with Jalview v.2.11.1.3 [59] using the Clustal color scheme.

281 3. Results

282 3.1. TE diversity, substitution levels and abundance

283 The longest 341 contigs from 95 fosmids (Figure S1), providing a total of 2,39
284 Mbp-2,55 Mbp with an average length of 7,657bp-7,472 bp and a median of 4,242-
285 4390bp (Table S3A & S3B) were further analyzed for TE and gene content (Figure 2).
286 Details on potentially overlapping contigs are provided in Table S4.

287

288

289

290

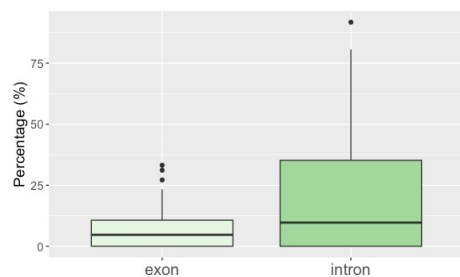
291

292

293

294

295



Deleted: 51

Deleted: 52

Deleted: 4

Deleted: 54

Deleted: 55

Deleted: 5

Deleted: 56

Deleted: 57

Deleted: 58

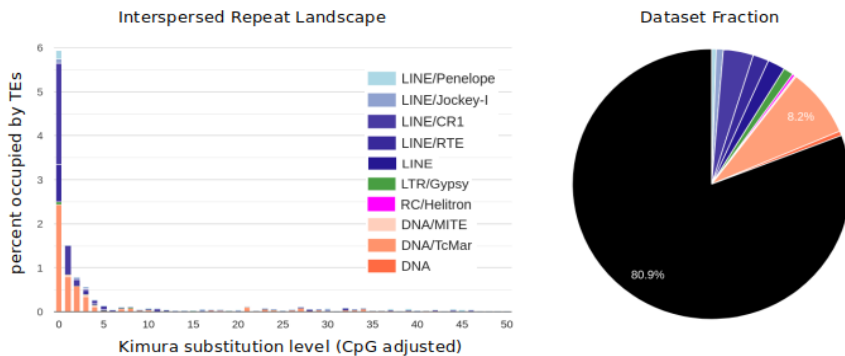
Deleted: <object>

Deleted: 2

307 **Figure 2: Box plots of intron and exon abundance.** The frequency of introns and
 308 exons were calculated as % of total fosmid lengths. Boxes contain the interquartile
 309 range from the 25th to the 75th percentile, the horizontal line indicates the median,
 310 and vertical lines minimum and maximum distributions of the data. Outliers are
 311 shown by dots.

312
 313 Our analyses revealed a high diversity of TEs in the selected clones from the
 314 fosmid library of *D. stevensoni* and the Illumina draft genome [45], including LINE-
 315 like retrotransposons, LTR retrotransposons, various cut-and-paste DNA
 316 transposons and Helitrons (Figure 3). DNA transposons were best represented at
 317 8.9% in the fosmids and 11.8% in the Illumina data, and belonged to Tc/mariner
 318 (most abundant at 8% in both datasets), hAT, Ginger, Merlin, Harbinger, and CMC-
 319 like DNA transposons, plus some uncharacterized DNA transposons. Similarly, for
 320 retrotransposons we found five major superfamilies of LINE-like elements (Jockey/I,
 321 CR1, L2, R4, RTE) with a total abundance of 4.2% and 2.8% in the fosmid and
 322 Illumina data, respectively, as well as gypsy-like (1%), Penelope-like elements (0.3%)
 323 and other unassigned retrotransposons (<0.1%) in the fosmids. Additionally, 4.2% of
 324 the sequence data were classified as non-LTR by Censor (Table S5), while Helitrons
 325 constituted 0.3% of the fosmid and 1.5% of the genomic sequence data. The high
 326 diversity of TEs in the fosmid data is also illustrated in 38 selected contigs containing
 327 mariner-1 (Figure 5a) and mariner-2 DNA TEs (Figure 5c, d), a mixture of DNA,
 328 LINE-like and LTR TEs (Figure 5b), and LINE-like RTE (Figure 5e) and CR1 (Figure
 329 5f) TEs.

330



331
 332
 333
 334
 335
 336
 337

Deleted: of fosmid size (a) and
 Deleted: of introns and exons
 Deleted: (b). The size range of fosmids is provided in basepairs (bp). ...

Deleted: ,

Deleted:

Deleted: .2

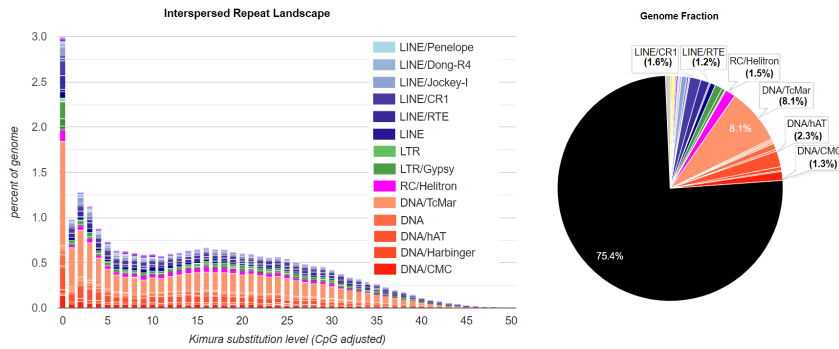
Deleted: , even though only the mariner probe was used for selection (Table S1 and S2)

Formatted: Highlight

Commented [MOU3]: Irina, could you please advise if we should also report these numbers from the genome data as they are not visible in new Figure 3b or leave them out?

Deleted: DNA

Formatted: Highlight



348 **Figure 3: Landscape divergence plots (left hand side) and genome occupancy by**
 349 **known TEs (right hand side) in *D. stevensoni*.** Divergences were calculated as
 350 Kimura substitution levels with adjusted CpG. Genome fraction of TEs was
 351 calculated after merging Repeat Masker and Censor outputs.
 352 (a, top) TEs in fosmid DNA sequence data. Genome fraction of TEs was calculated
 353 after merging Repeat Masker and Censor outputs. (b, bottom) TEs in the preliminary
 354 draft genome assembly [45]. The plot was constructed using the REPET library
 355 obtained with the Illumina assembly. The pie chart shows genome occupancy for TE
 356 categories occupying more than 1% of the genome.

Deleted: fosmid DNA sequence data of

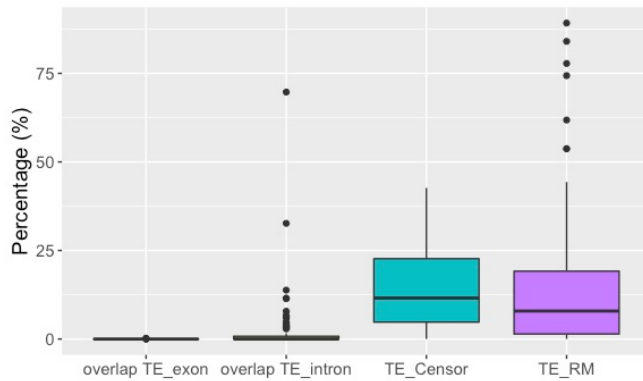
Deleted:

Formatted: Font: Bold

357
 358
 359 The distribution of Kimura substitution levels on the TE divergence plot was
 360 negatively logarithmic in both data sets (Figure 3a & 3b), with most TEs having low
 361 substitution levels and only a few TEs showing high levels of substitution, indicating
 362 that most copies originated from relatively recent transposition events. In total,
 363 19.1% of all fosmid DNA sequence data (Figure 3a) and 25.6% of the draft genome
 364 (Figure 3b) comprised (known) TE sequences. Repeat Masker and Censor estimated
 365 the median frequencies of TEs per fosmid as 8.6%-9.4% and 11.7%-12.8%,
 366 respectively, and average frequencies of 16.6%-17.5% and 16.0%-16.7%, respectively
 367 (Figure 4 and Table S3B). Average TE abundance estimated at the contig level was
 368 similar, with 13.7%-14.7% (Repeat Masker) and 16.5%-16.9% (Censor; Table S3A).
 369

Formatted: Indent: First line: 0 cm

Deleted: (Figure 3)



373
 374 **Figure 4: Box plots of TE abundance and overlap of TEs with exons and introns in**
 375 **fosmid data.** TEs were identified with Censor from translated fosmid DNA
 376 sequences. All frequencies were calculated as % of total fosmid lengths. Boxes
 377 contain the interquartile range from the 25th to the 75th percentile, the horizontal line
 378 indicates the median, and vertical lines minimum and maximum distributions of the
 379 data. Outliers are shown by dots.

380 3.2. TE insertion sites in fosmids and their relationship to telomeres and coding regions

381 When comparing hybridization signals, there was no overlap between fosmids
 382 with a signal for telomeres and fosmids that contained TEs. With regard to coding
 383 regions, fosmids contained on average 6.4%-6.7% exons and 20.1% introns, with a
 384 maximum of 91.2% introns (Figure 2).

385 The second set of 11 fosmids that had been selected with probes for nuclear
 386 genes contained more exons and introns than the other fosmids (Figure S2). Most
 387 TEs were not located in exons or introns, as is obvious from Figure 4 and shown in
 388 detail in Tables S3A & B. While on average only 0.01% of TEs overlapped with exons,
 389 there was limited overlap between TEs and introns (Figure 4) with an average of
 390 2.0%-2.1% for all fosmids and 9.8% for the second set of 11 fosmids (Figure S2). The
 391 medians for both features were 0 and 0-0.5%, respectively (Figure 4). The minimal
 392 overlap between TEs and coding regions is also visible in the sequence features of
 393 fosmids, of which 38 examples are visualized in Figure 5. The BUSCO analyses
 394 retrieved 23 complete BUSCO genes, of which 19 were single-copy and four
 395 duplicated, and an additional nine fragmented genes; 98.8% of the searched 2675
 396 arthropod BUSCO genes were missing. Thus, in terms of core arthropod genes, the
 397 analyzed set of sequences does not comprise particularly gene-poor regions,
 398 representing about 1% of core genes, while it constitutes only ~0.35% of total
 399 genomic DNA as measured by flow cytometry/DAPI staining.

400 3.3. Additional domains in *R4/Dong* and *Gypsy* retrotransposons

401 While the majority of complete or nearly complete DNA and RNA TEs revealed
 402 the expected domain architectures, two retrotransposon families, *R4/Dong* and

Deleted: 1

Deleted: seen

Deleted: in

Deleted: 1

Deleted: six

408 *Gypsy* (Figures 5b and 6), deserve special mention. Members of the R4/Dong clade
409 of non-LTR retrotransposons contain the reverse transcriptase and REL-
410 endonuclease domains and insert into rDNA or into microsatellite targets. However,
411 no recognizable motifs could be previously distinguished at their N-terminus, in
412 contrast to rDNA-specific R2 retrotransposons with a similar REL-endonuclease
413 which harbor an N-terminal Myb DNA-binding domain [60-64]. We aligned two
414 *Dong* representatives with a full-length ORF from contigs 45 and 333 (Figure 5b) and
415 a set of diverse R4/*Dong*-like elements from cnidarians, mollusks, insects, fish and
416 nematodes, and used HHpred [62] to uncover a highly diverged SANT/Myb-like
417 domain close to the N-terminus (Figure 6a), with the best scores obtained from
418 rDNA-specific R4 elements of nematodes (94.9% probability hit to PF16282.6 for
419 *Ancylostoma caninum*). In the well-studied rDNA-specific R2 clade, this domain
420 reportedly directs site-specific insertion into rDNA, along with accompanying Zn-
421 finger motifs [63]. Thus, it may be argued that the divergent Myb version found in
422 *Dong*-like elements is similarly responsible for site-specific integration, albeit in the
423 absence of Zn-finger motifs at the N-termini. In *D. stevensoni*, the *Dong* insertion
424 target is represented by (TAA)_n repeats, as is the case in most insects, mollusks and
425 cnidarians, and is therefore located outside coding sequences.

426 The structure of *Gypsy*-like LTR-retrotransposons is similar to that of
427 retroviruses, with the *gag* gene encoding a nucleocapsid and the *pol* gene encoding
428 protease, reverse transcriptase and integrase enzymatic domains [28]. Inspection of
429 the nearly complete *Gypsy_Ds1* on contig 89 (Figure 5b) reveals an atypical 250-aa
430 extension beyond the integrase domain, which typically ends with a GPY/F motif,
431 but may contain an additional chromodomain at the extreme C-terminus. However,
432 in the C-terminal extension of *Gypsy_Ds1 pol*, HHpred identified remote similarity
433 to the trimeric coiled-coil domains of spike proteins from enveloped +ssRNA viruses
434 (coronaviruses) and dsRNA viruses (reoviruses) (Figure 6b) [65-67]. Although it also
435 carries a potential furin-like protease cleavage site (RxxR), this extension domain is
436 too short to represent a fully functional *env* (~600 aa), which is responsible for
437 interaction with host membranes during viral entry and egress and is often found in
438 LTR-retrotransposons as the third ORF [67]. Rather, it may be a remnant of an
439 original *env* which was captured from an RNA virus and used for initial horizontal
440 entry into the *D. stevensoni* host. Possible *env*-like ORF3 remnants were found in
441 *Vesta* LTR-retrotransposons in the bdelloid rotifer *Adineta vaga* [69]. However, it is
442 also possible that the C-terminal extension is unrelated to *env*, and the coiled-coil
443 domain could instead be used for interaction of integrase with other proteins.

444

Deleted: 59

Deleted: 63

Deleted: 61

Deleted: knuckle

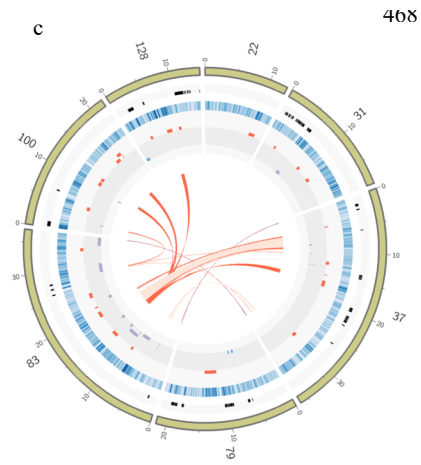
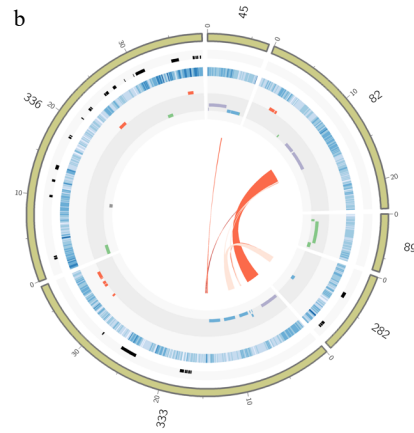
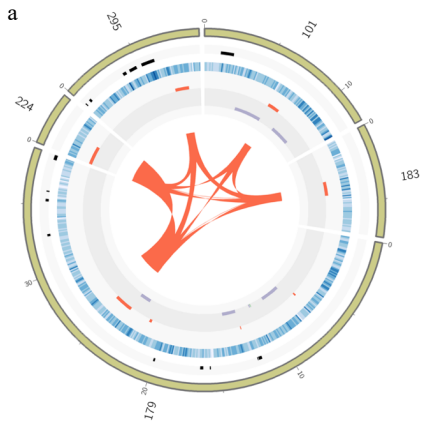
Deleted: 62

Deleted: knuckle

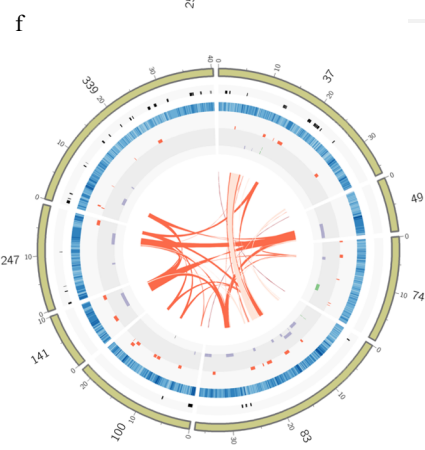
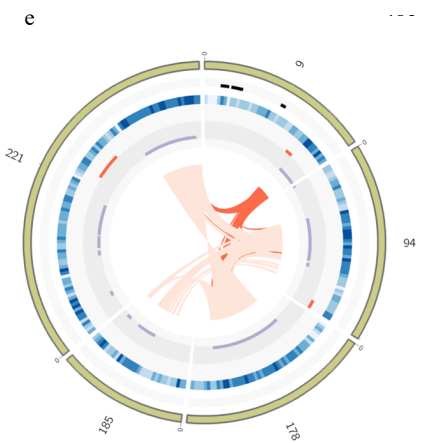
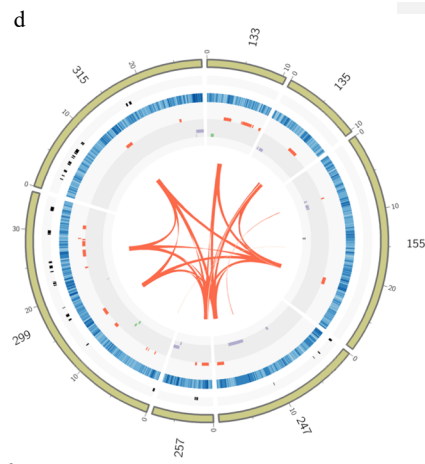
Deleted: 64

Deleted: 66

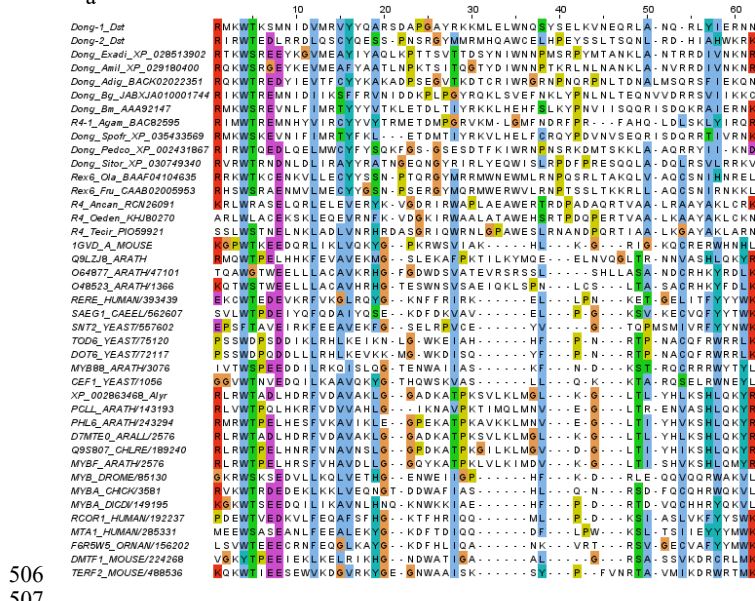
Deleted: 68



408



487 **Figure 5: Sequence features of representative fosmid contigs.** Features of contigs
 488 (marked outside in yellow) are plotted on tracks **and their identities indicated as**
 489 **coloured boxes in the figure legend.** Shades of red represent % identity from BLAST
 490 searches (dark color 100%, intermediate 90-99%, and light color 80-89%), indicating
 491 recent transposition (see also Table S4). Large numbers on the outside indicate
 492 contigs; smaller numbers, the position in kb. Translated TEs were identified with
 493 Censor; transcripts, exons and introns were predicted with Augustus; and all
 494 features visualized with Circos. For further details on contigs, see Table S3A.
 495 5a: Contigs Ds_ctg224, Ds_ctg295, Ds_ctg101, Ds_ctg183 & Ds_ctg179 containing
 496 mariner-1 DNA TEs. 5b: Contigs Ds_ctg 45, Ds_ctg 82, Ds_ctg 89, Ds_ctg 282, Ds_ctg
 497 333 & Ds_ctg 336 with various TEs including DNA (mariner), LINE (PLE and CR1),
 498 and LTR (gypsy). 5c and 5d: Contigs Ds_ctg22, Ds_ctg31, Ds_ctg37, Ds_ctg79,
 499 Ds_ctg83, Ds_ctg100 & Ds_ctg128 and Ds_ctg133, Ds_ctg135, Ds_ctg155, Ds_ctg247,
 500 Ds_ctg257, Ds_ctg299 & Ds_ctg315, respectively, displaying abundant mariner-2
 501 TEs with high sequence similarities. 5e and 5f: Contigs containing LINE-like TEs,
 502 including contigs Ds_ctg9, Ds_ctg94, Ds_ctg178, Ds_ctg185 and Ds_ctg221
 503 containing RTE (Fig. 5e) and contigs Ds_ctg37, Ds_ctg49, Ds_ctg74, Ds_ctg83,
 504 Ds_ctg100, Ds_ctg141, Ds_ctg247 & Ds_ctg339 containing CR1 (Fig. 5f) TEs.



506
507
508
509
510
511
512

Formatted: Highlight

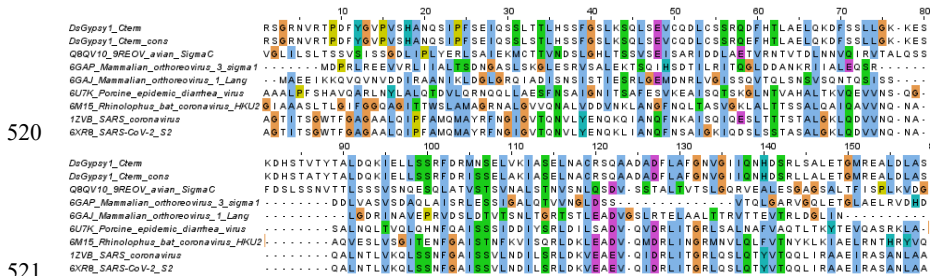
Formatted: Highlight

Deleted: showing, in the inward direction, the positions of exons (in black), GC content (in %, light blue), DNA TEs (in red), LINE TEs (in purple), Penelope-like TEs (in blue), LTR TEs (in green) and other TEs (in grey).

Deleted: hown in s

Deleted: is

Deleted: the



520 **Figure 6:** Regions of homology in *R4/Dong* (6a) and *Gypsy* (6b) retrotransposons of *D. stevensoni*. Multiple sequence alignments were visualized with Jalview [59].

524 6a: Alignment includes *Dong1* and *Dong2* (*D. stevensoni*) and related elements from
 525 cnidarians (*Exaiptasia diaphana*, *Acropora millepora*, *Acropora digitata*), mollusks
 526 (*Biomphalaria glabrata*), insects (*Bombyx mori*, *Anopheles gambiae*, *Spodoptera frugiperda*,
 527 *Pediculus humanus corporis*, *Sitophilus oryzae*), fish (*Oryzias latipes*, *Takifugu rubripes*)
 528 and nematodes (*Ancylostoma caninum*, *Oesophagostomum dentatum*, *Teladorsagia*
 529 *circumcincta*) with the corresponding accession numbers, followed by a
 530 representative selection of Myb-like domains from the PF00249 seed alignment (25
 531 out of 147). 6b: Structure-based alignment of *D. stevensoni Gypsy1* C-terminus
 532 (amino acids 1322-1479 out of 1486) and the central helix domain of the spike (sigma)
 533 proteins from reoviruses and coronaviruses identified by HHpred, with the
 534 corresponding PDB accession numbers.

535 **4. Discussion**

536 **4.1. TE diversity and substitution levels**

537 Our results show a high diversity of transposons in the genome of the putative
 538 ancient asexual ostracod *D. stevensoni* from both, fosmid library and draft genome
 539 data (Figure 3 a, b and Figure 5). Compared to studies in another presumed anciently
 540 asexual taxon, bdelloid rotifers, the genome of the ostracod *D. stevensoni* seems to
 541 have a higher TE proportion for all major transposon groups. Given the
 542 exceptionally low transposable element load in bdelloids, especially for LINE-like
 543 elements [10,13,14], this result could be expected. Two species of putative ancient
 544 asexual oribatid mites, for which TE data are also available [18], contained similar
 545 levels of diversity as observed in the current study. In all three groups of putative
 546 ancient asexuals, the majority of TEs were DNA transposons (Figure 3 a, b and 5;
 547 [10,13,14,18]), however this was not the case for the (younger) asexual *Daphnia*
 548 [17,70,71] and *Meloidogyne* nematodes [72]. The higher abundances of DNA
 549 transposons in putative ancient asexuals can probably best be explained by their
 550 prevailing transmission mode, which is often horizontal [31,73-75], and thus
 551 potentially less influenced by long-term loss of meiosis and sex. In aquatic habitats
 552 where the ostracod *D. stevensoni* occurs, horizontal transmission of TEs seems to be
 553 more common than in terrestrial habitats, because DNA is not exposed to UV or dry
 554 air [76].

Deleted: 58

Deleted: Its actual TE diversity is expected to be even higher, given that REPET, which is designed for analyses of whole-genome data, takes into account only transposons with at least three copies, while TEs occurring in the dataset once or twice could be detected only at the protein level by Censor.

Deleted: 69

Deleted: 70

Deleted: 71

Deleted: 72

Deleted: 74

Deleted: 75

568 The low number of nucleotide substitutions in TEs that was observed in the
 569 current study from both fosmid and genome data (Figure 3 a, b) indicates that the
 570 majority of TEs in the genome of *D. stevensoni* have been recently active; similar
 571 patterns were described for the putative ancient asexual bdelloid rotifer *A. vaga* [76].
 572 The study of Bast *et al.* [18] revealed higher levels of nucleotide substitutions in TEs
 573 of oribatid mites, inconsistent with recent activity. Since it is unclear if the
 574 methodologies of [18] were fully equivalent to the analyses conducted here and to
 575 [77], these differences will not be further discussed. Active transposition seems
 576 generally to be widespread in both animal and plant genomes [78], but uncontrolled
 577 copy number increase can be counteracted by genome defense systems, DNA decay
 578 and loss, and negative selection.

579 4.2. TE abundance

580 Eukaryotic genomes can differ drastically in their genomic TE content, ranging
 581 from a few per cent to over 80% [79]. With an estimate of 19.1% (Figure 3) for all
 582 fosmid data, the transposable load in our fosmid DNA sequence data is slightly
 583 lower than the estimated TE abundance of *D. stevensoni* at the whole genome level
 584 (Figure 3b). This discrepancy can be explained by the fact that the Illumina repeat
 585 library showed about 5% higher TE content due to the addition of more divergent
 586 TE regions, which were only partially covered by Censor. While final conclusions
 587 on the transposon abundance in *D. stevensoni* should be deferred until high quality,
 588 genome-wide data from long read technologies become available, a transposable
 589 load of up to 26% (of known TEs) would be in the range of TE loads in other
 590 arthropods. In insects, TE abundances range from 6 up to 58% [80]. In aquatic
 591 crustaceans other than ostracods, such as crabs and shrimps, repeats and TEs can
 592 make up between 50.4% and 57% [81-83] of the genome, although TE content from
 593 7.4% to 12.9% was reported for different assemblies of *Daphnia pulex* [17,70,71]. In
 594 other, probably younger, asexuals, TE content at the genome-wide scale can exceed
 595 50%, as for example in *Meloidogyne* root-knot nematodes [72].

596 4.3. TE insertion sites

597 One of the possible explanations for the relatively high TE content of *D.*
 598 *stevensoni* in our sequence data could be their genomic locations. Through partial
 599 selection of fosmids containing transposons, we might have sequenced some TE
 600 islands in the genome of *D. stevensoni* outside of coding regions. Our results
 601 detecting up to 19.4% exons in individual fosmids but only an average overlap of up
 602 to 0.01% between exons and TE and up to 2.1% between introns and TEs in the
 603 boxplot (Figure 4) support this point of view; and are illustrated for 38 selected
 604 fosmids in Figure 5a-f. These observed patterns would largely be consistent with
 605 predictions [79] on the predominantly neutral character for the bulk of TE insertions,
 606 but will require genome-wide data for confirmation. The available Illumina draft
 607 genome of *D. stevensoni* is too fragmented [45] to test these assumptions further.

608

Deleted: 76

Deleted: 77

Deleted: 78

Deleted: data

Deleted: probably

Deleted: comparable to the

Deleted: , given that only 13 out of 104 fosmids were selected with TE-specific probes (Table S2).

Deleted: 19.1

Deleted: %

Deleted: 79

Deleted: 80

Deleted: 82

Deleted: 69

Deleted: 70

Deleted: 71

Deleted: (biased)

Deleted:

Deleted: also

Deleted: (Figure 4 and

Deleted:)

Deleted: 78

Deleted: ,

Deleted: .

Formatted: Font: Italic

Formatted: Font:

633 Both, the draft genome of *D. stevensoni* as well as sequenced fosmids seem to
 634 harbor recently active transposons, as supported by the estimated low substitution
 635 levels indicating recent activity (Figure 3) and from overlapping TE-rich regions of
 636 fosmid contigs (see examples in Figure 5a-f). These indications for relatively recent
 637 transposition, together with the low number of insertions within exons (Figure 4), at
 638 least partly fit the dichotomous pattern that Muszewska *et al.* described from fungal
 639 transposons [84], where young TEs were not located inside genes, while older TEs
 640 were found both inside and outside of coding regions. It is also possible that the
 641 sequenced TE islands of *D. stevensoni* in the fosmid dataset could come from
 642 pericentromeric regions, given that we did not sequence any fosmids containing
 643 telomeres. Other studies on humans [85] and rice [86], for example, found a higher
 644 abundance of TEs near centromeres. The lack of LINE-like TEs being associated with
 645 telomeres in *D. stevensoni* in fosmid sequence data also indicates that there has been
 646 no co-option of the investigated TEs for telomeric functions, as in *Drosophila* [87] or
 647 bdelloid rotifers [88].

Deleted: The genomic regions of

Deleted: here

Deleted: 83

Deleted: our

Deleted: 84

Deleted: 85

Formatted: Font: Not Italic

Deleted: 86

Deleted: 87

648 4.4. Assessing the impact of putatively ancient asexual reproduction on TE landscapes in non- 649 marine ostracods

650 Following one of the predictions outlined in the introduction, long-term
 651 asexuality is expected to increase the transposable element load because of reduced
 652 efficiency of selection for the removal of deleterious mutations and transposons in
 653 finite populations [4,5,6]. Our results are consistent with this hypothesis. It is
 654 possible that asexual darwinulid ostracods inherited relatively high transposable
 655 loads from their sexual ancestors when abandoning sexual reproduction, which
 656 could go back as far as 200 myr ago [37] and to 25 Mya in *D. stevensoni* [38]. Glémin
 657 *et al.* implied that it might take a long time for asexuals to purge TEs from their
 658 genomes [25]. Our results indicate that even millions of years have not been
 659 sufficient for some Darwinulidae to efficiently purge their TE.

660 Unrestrained TE proliferation should eventually drive asexual lineages to
 661 extinction, unless asexual hosts can tightly control TE copy numbers [10-12], with
 662 putative ancient asexual bdelloids as the most striking example [10,13,14].
 663 Eukaryotic hosts have developed a wide arsenal of molecular defense mechanisms
 664 against TEs [29,89], including for example siRNAs and piRNAs [90,91], and
 665 chromatin-based pathways [92]. The relatively high TE content and diversity in *D.*
 666 *stevensoni* could imply that some of these defense mechanisms are lacking or are less
 667 efficient, leading to the accumulation of transposons when these are not removed
 668 [25]. This explanation seems more likely than the lack of time for purging TEs from
 669 sexual ancestors. Alternatively, the insertion pattern of TEs in *D. stevensoni*, as
 670 suggested by our preliminary observations, may be biased towards non-coding
 671 regions, and could therefore have less deleterious effects on the host. The observed
 672 lack of insertions into exons as observed in the fosmid data is most likely explained
 673 by selection against genic insertions. Finally, certain TEs, such as *Dong*, display
 674 insertion specificity that directs them away from coding regions.

Deleted: 88

Deleted: 89

Deleted: 90

Deleted: 91

687 Another factor that can potentially influence transposon abundance is the
 688 presence of bacterial endosymbionts. Kraaijeveld et al. suggested that the higher
 689 copy numbers of *gypsy* transposons in asexual wasps as compared to sexual relatives
 690 [23] could partly be due to the feminizing endosymbiont *Wolbachia*, which is only
 691 present in asexuals. The *Cardinium* endosymbionts, which could have similar effects
 692 on their hosts as *Wolbachia*, have recently been described in non-marine ostracods
 693 including *D. stevensoni* [93], but their potential effect on transposable element loads
 694 in asexual ostracods remains to be investigated.

695 Our results based on an Illumina draft genome [45] and parts of a fosmid library
 696 indicate that asexual reproduction in the ostracod *D. stevensoni* did not substantially
 697 reduce its transposable load, as may have been the case in other asexual taxa
 698 [3,10,11,13,15,16,73]. On the contrary, it rather seems that this ostracod species is
 699 another example of an asexual being less efficient in removing TEs. Whether this is
 700 owing to the loss or dysfunction of molecular defense mechanisms controlling TE
 701 abundance, the absence of methylation, preferred insertion outside of coding
 702 regions, or other factors, remains to be investigated in future studies when
 703 comparative genomic and transcriptomic data of high quality for this and other
 704 ostracod species become available. The absence of sex in darwinulid ostracods has
 705 been estimated from fossil data to be as old as 25 myr (*D. stevensoni* [38]) up to 200
 706 myr (the entire post-Palaeozoic family Darwinulidae, using *Alicenula* as proxy [37]),
 707 and many asexual darwinulids became extinct after the Permian-Triassic [94]. The
 708 fact that about 30 putative ancient asexual darwinulid species are still present today
 709 suggests that TE proliferation has not driven all of these species to extinction, as
 710 might be expected [11,12]. Comparisons with TE abundance in sexual ostracods and
 711 younger asexual species are required to test whether the observed patterns of TE
 712 abundance and diversity are general features related to the old age of Ostracoda of
 713 more than 400 myr [95] or to ancient asexuality of the Darwinulidae.

714 **Supplementary Materials:** The following are available online at www.mdpi.com/xxx/s1, Figure S1: Box plot of
 715 size distribution of analysed contigs from the fosmid library. Size of sequenced contigs. Figure S2: Comparison
 716 of sequence features between three groups of fosmids. Table S1: Probes used for hybridization and detection of
 717 fosmids containing TE or telomeres. Table S2: Hybridization signal of selected fosmids for sequencing. Table
 718 S3A: Contig sequence features. Table S3B: Fosmid sequence features. Table S4: Overview of possible overlap
 719 between contig ends. Table S5: Results of TE identification with Censor.

720 **Author Contributions:** Conceptualization, I.S. and I.A.; methodology, F.R. and I.A.; software, F.R.; validation,
 721 I.S., F.R., M.D. and I.A.; formal analysis, I.S., F.R., M.D. and I.A.; investigation, I.S., K.M. and I.A.; resources, I.S.
 722 and K.M.; data curation, I.S., I.A. and F.R.; writing—original draft preparation, I.S.; writing—review and editing,
 723 I.S., F.R., K.M., M.S. and I.A.; visualization, I.S., F.R., M.S. and I.A.; supervision, F.R. and I.A.; project
 724 administration, I.S.; funding acquisition, I.S., K.M. All authors have read and agreed to the published version of
 725 the manuscript.

726 **Funding:** This research was funded by Belgian Federal Science Policy (Belspo), grant number WI/36/103. The
 727 stay of IS at Woods Hole was funded by the L. & A. Colwin Fund of the Marine Biology Laboratory, MA. MD
 728 was supported by the Blue Economy Internship Program (BEIP) of the Commonwealth of Massachusetts at the
 729 MBL.

730 **Acknowledgments:** Irina Yushenova (Woods Hole, USA) is acknowledged for helpful suggestions with the
 731 analyses, Andy Vierstraten (Gent, Belgium) and Arnaud Bellec (CNRGV, INRA, Toulouse, France) and his
 732 colleagues for technical support with fosmid sequencing, Marie Cours (Brussels, Belgium) for assistance in

Deleted: 92

Deleted: Although o

Deleted: data

Deleted: do not extend to a genome-wide scale,

Deleted: they

Deleted: 72

Deleted:

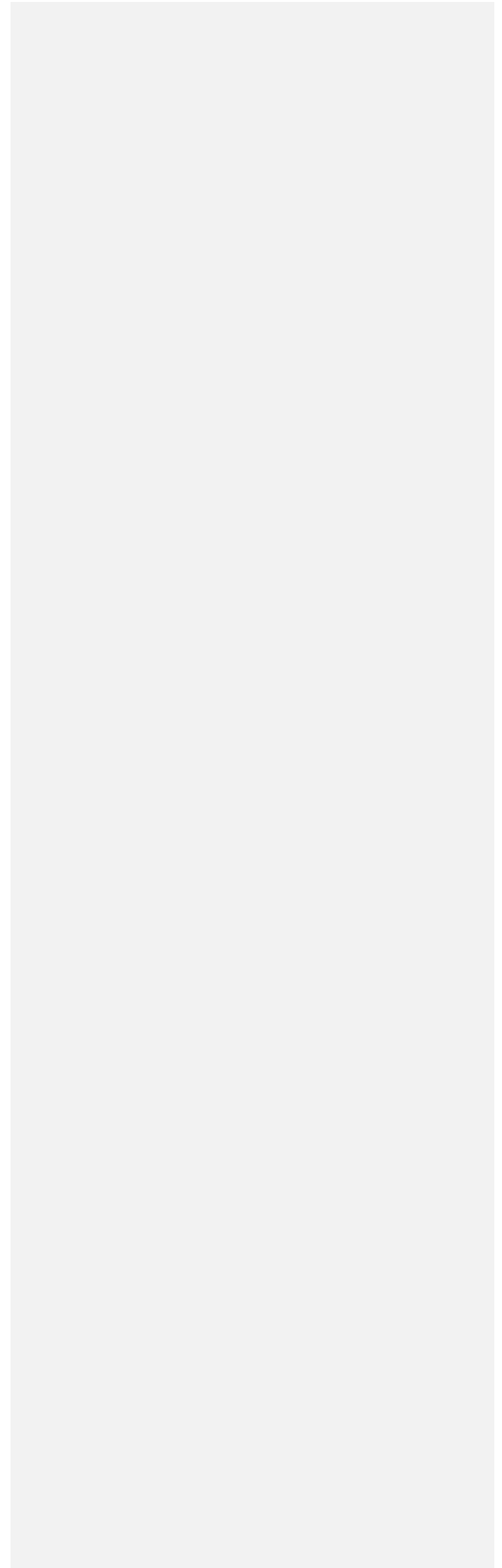
Deleted: 93

Deleted: 94

742 drawing the box plots, and Jeroen Venderickx (Brussels, Belgium) for providing the photograph of the *D.*
743 *stevensoni* sample.

744 **Conflicts of Interest:** The authors declare no conflict of interest. The funders had no role in the design of the
745 study; in the collection, analyses, or interpretation of data; in the writing of the manuscript, or in the decision to
746 publish the results.

747



748 **References**

749

- 750 1. Hickey, D.A. Selfish DNA: a sexually-transmitted nuclear parasite. *Genetics*, **1982**, *101*, 519–531.
- 751 2. Zeyl, C., Bell, G., Green, D.M. Sex and the spread of retrotransposon Ty3 in experimental
752 populations of *Saccharomyces cerevisiae*. *Genetics*, **1996**, *143*, 1567–1577.
- 753 3. Bast, J., Jaron, K.S., Schuseil, D., Roze, D., Schwander, T. Asexual reproduction reduces
754 transposable element load in experimental yeast populations. *eLife*, **2019**, *8*, e48548.
755 doi:10.7554/eLife.48548
- 756 4. Kondrashov, A.S. Deleterious mutations and the evolution of sexual reproduction. *Nature*, **1988**,
757 *336*, 435–440.
- 758 5. Muller, H.J. The relation of recombination to mutational advance. *Mutat. Res.*, **1964**, *1*, 2–9.
- 759 6. Dolgin, E.S., Charlesworth, B. The fate of transposable elements in asexual populations. *Genetics*,
760 **2006**, *174*, 817–827. 10.1534/genetics.106.060434
- 761 7. Bachtrog, D. Y-chromosome evolution: emerging insights into processes of Y-chromosome
762 degeneration. *Nat. Rev. Genet.*, **2013**, *14*, 113–124. <https://doi.org/10.1038/nrg3366>
- 763 8. Leung, W., Shaffer, C.D., Reed, L.K., Smith, S.T., Barshop, W., Dirkes, W., Dothager, M., Lee, P.,
764 Wong, J., Xiong, D., et al. *Drosophila* Muller F elements maintain a distinct set of genomic
765 properties over 40 million years of evolution. *G3*, **2015**, *5*, 719–7440. 10.1534/g3.114.015966
- 766 9. Lynch, M., Blanchard, J.L. Deleterious mutation accumulation in organelle genomes. *Genetica*,
767 **1998**, *102–103*, 29–39. <https://doi.org/10.1023/A:1017022522486>
- 768 10. Arkhipova, I., Meselson, M. Transposable elements in sexual and ancient asexual taxa. *Proc. Natl.*
769 *Acad. Sci. U.S.A.*, **2000**, *97*, 14473–14477. <https://doi.org/10.1073/pnas.97.26.14473>
- 770 11. Arkhipova, I., Meselson, M. Deleterious transposable elements and the extinction of
771 asexuals. *Bioessays*, **2005**, *27*, 76–85. 10.1002/bies.20159
- 772 12. Nuzhdin, S.V., Petrov, D.A. Transposable elements in clonal lineages: lethal hangover from sex.
773 *Biol. J. Linn. Soc.*, **2003**, *79*, 33–41.
- 774 13. Flot, J.F., Hespels, B., Li, X., Noel, B., Arkhipova, I., Danchin, E.G., Hejnol, A., Henrissat, B.,
775 Koszul, R., Aury, J.M., et al. Genomic evidence for ameiotic evolution in the bdelloid rotifer
776 *Adineta vaga*. *Nature*, **2013**, *500*, 453–457. <https://doi.org/10.1038/nature12326>
- 777 14. Arkhipova, I.R., Meselson, M. Diverse DNA transposons in rotifers of the class Bdelloidea. *Proc.*
778 *Natl. Acad. Sci. U.S.A.*, **2005**, *102*, 11781–11786. <https://doi.org/10.1073/pnas.0505333102>
- 779 15. Schaack, S., Pritham, E.J., Wolf, A., Lynch, M. DNA transposon dynamics in populations of
780 *Daphnia pulex* with and without sex. *Proc. R. Soc. B.*, **2010**, *277*, 2381–
781 2387. <https://doi.org/10.1098/rspb.2009.2253>
- 782 16. Rho, M., Schaack, S., Gao, X., Kim, S., Lynch, M., Tang, H. LTR retroelements in the genome of
783 *Daphnia pulex*. *BMC Genomics*, **2010**, *11*, 425. 10.1186/1471-2164-11-425
- 784 17. Jiang, X., Tang, H., Ye, Z., Lynch, M. Insertion polymorphisms of mobile genetic elements in
785 sexual and asexual populations of *Daphnia pulex*. *Genome Biol. Evol.*, **2017**, *9*, 362–374.
786 <https://doi.org/10.1093/gbe/evw302>
- 787 18. Bast, J., Schaefer, I., Schwander, T., Maraun, M., Scheu, S., Kraaijeveld, K. No accumulation of
788 transposable elements in asexual arthropods. *Mol. Biol. Evol.*, **2016**, *33*, 697–706. doi:
789 10.1093/molbev/msv261
- 790 19. Szitenberg, A., Cha, S., Opperman, C.H., Bird, D.M., Blaxter, M.L., Lunt, D.H. Genetic drift, not
791 life history or RNAi, determine long-term evolution of transposable elements. *Genome Biol. Evol.*,
792 **2016**, *8*, 2964–2978. 10.1093/gbe/evw208
- 793 20. Agren, J.A., Greiner, S., Johnson, M.T., Wright, S.I. No evidence that sex and transposable
794 elements drive genome size variation in evening primroses. *Evolution*, **2015**, *69*, 1053–1062.
795 <https://doi.org/10.1111/evo.12627>
- 796 21. Zeyl, C., Bell, G., Dasilva, J. Transposon abundance in sexual and asexual populations
797 of *Chlamydomonas reinhardtii*. *Evolution*, **1994**, *48*, 1406–1409. 10.2307/2410398
- 798 22. Abad, P., Gouzy, J., Aury, J.-M., Castagnone-Sereno, P., Danchin, E.G.J., Deleury, E., Perfus-
799 Barbeoch, L., Anthouard, V., Artiguenave, F., Blok, V.C. et al. Genome sequence of the metazoan

- 800 plant-parasitic nematode *Meloidogyne incognita*. *Nat. Biotechnol.*, **2008**, *26*, 909–915.
801 <https://doi.org/10.1038/nbt>. Abad, P., Gouzy, J., Aury, J.-M., Castagnone-Sereno, P., Danchin,
802 E.G.J., Deleury, E., Perfus-Barbeoch, L., Anthouard, V., Artiguenave, F., Blok, V.C. et al. Genome
803 sequence of the metazoan plant-parasitic nematode *Meloidogyne incognita*. *Nat. Biotechnol.*, **2008**,
804 *26*, 909–915. <https://doi.org/10.1038/nbt.1482>
- 805 23. Kraaijeveld, K., Zwanenburg, B., Hubert, B., Vieira, C., De Pater, S., Van Alphen, J.J.M., Den
806 Dunnen, J.T., De Knijff, P. Transposon proliferation in an asexual parasitoid. *Mol. Ecol.*, **2012**, *21*,
807 3898–3906. 10.1111/j.1365-294X.2012.5582
- 808 24. Simonti, C.N., Pavlicev, M., Capra, J.A. Transposable element exaptation into regulatory regions
809 is rare, influenced by evolutionary age, and subject to pleiotropic constraints. *Mol. Biol. Evol.*,
810 **2017**, *34*, 2856–2869. doi:10.1093/molbev/msx219
- 811 25. Glémin S, François CM, Galtier N. Genome Evolution in Outcrossing vs. Selfing vs. Asexual
812 Species. *Methods Mol. Biol.*, **2019**, *1910*, 331–369. doi: 10.1007/978-1-4939-9074-0_11
- 813 26. Charlesworth, B., Langley, C. The evolution of self-regulated transposition of transposable
814 elements. *Genetics*, **1986**, *112*, 359–383.
- 815 27. Startek, M., Le Rouzic, A., Capy, P., Grzebelu, D., Gambin, A. Genomic parasites or symbionts?
816 Modeling the effects of environmental pressure on transposition activity in asexual populations.
817 *Theor. Popul. Biol.*, **2013**, *90*, 145–151. <https://doi.org/10.1016/j.tpb.2013.07.004>
- 818 28. Arkhipova, I.R. Using bioinformatic and phylogenetic approaches to classify transposable
819 elements and understand their complex evolutionary histories. *Mobile DNA*, **2017**, *8*, 19.
820 doi:10.1186/s13100-017-0103-2
- 821 29. Bourque, G., Burns, K.H., Gehring, M., Gorbunova, V., Seluanov, A., Hammell, M., Imbeault,
822 M., Izsvák, Z., Levin, H.L., Macfarlan, T.S., Mager, D.L., Feschotte, C. Ten things you should
823 know about transposable elements. *Genome Biol.*, **2018**, *19*, 199. doi: 10.1186/s13059-018-1577-z
- 824 30. Huang, C.R., Burns, K.H., Boeke, J.D. Active transposition in genomes. *Ann. Rev. Gen.*, **2012**, *46*,
825 651–675. doi:10.1146/annurev-genet-110711-155616
- 826 31. Peccoud, J., Loiseau, V., Cordaux, R., Gilbert, C. Horizontal transfer of transposons in insects.
827 *Proc. Natl. Acad. Sci. U.S.A.*, **2017**, *114*, 4721–4726. 10.1073/pnas.1621178114
- 828 32. Schön, I., Rossetti, G., Martens, K. Ancient asexual darwinulids : ancient scandals or scandalous
829 gossip? In *Lost sex. The evolutionary biology of parthenogenesis*; Schön, I., Martens, K., Van Dijk,
830 Eds.; Springer Academic Publishers, Dordrecht, The Netherlands, 2009, pp. 217–240.
- 831 33. Heethoff, M., Norton, R.A., Scheu, S., Maraun, M. Parthenogenesis in oribatid mites
832 (Acari, Oribatida): evolution without sex In *Lost sex. The evolutionary biology of*
833 *parthenogenesis*; Schön, I., Martens, K., Van Dijk, Eds.; Springer Academic Publishers, Dordrecht,
834 The Netherlands, 2009, pp. 241–258.
- 835 34. Schwander, T. Evolution: The end of an ancient asexual scandal. *Curr. Biol.*, **2016**, *26*, R233–
836 235. 10.1016/j.cub.2016.01.034
- 837 35. Schwander, T., Lee, H., Crespi, B.J. Molecular evidence for ancient asexuality
838 in *Timema* stick insects. *Curr. Biol.*, **2011**, *21*, 1129–1134. 10.1016/j.cub.2011.05.026
- 839 36. Mark Welch, D., Ricci, C., Meselson, M. Bdelloid rotifers: progress in understanding the success
840 of an evolutionary scandal. In *Lost sex. The evolutionary biology of parthenogenesis*; Schön, I.,
841 Martens, K., Van Dijk, Eds.; Springer Academic Publishers, Dordrecht, The Netherlands, 2009,
842 pp. 259–280.
- 843 37. Martens, K., Rossetti, G., Horne, D. How ancient are ancient asexuals? *Proc. R. Soc. B*, **2003**, *270*,
844 723–729. <https://doi.org/10.1098/rspb.2002.2270>
- 845 38. Straub, E.B. Mikropaläontologische Untersuchungen im Tertiär zwischen Ehingen und
846 Ulm a.d. Donau. *Geol. Jb.*, **1952**, *66*, 433–523.
- 847 39. Schön, I., Arkhipova, I.R. Two families of non-LTR retrotransposons, *Syrinx* and *Daphne*, from
848 the Darwinulid ostracod, *Darwinula stevensoni*. *Gene*, **2006**, *371*, 296–307.
- 849 40. Shribak, M. Polychromatic polarization microscope: bringing colors to a colorless world. *Sci.*
850 *Rep.*, **2015**, *5*, 17340. <https://doi.org/10.1038/srep17340>

- 851 41. Tétart, J. Les garnitures chromosomiques des Ostracodes d'eau douce. *Trav. Lab. Hydrobiol. Univ. Grenoble*, **1978**, *69-70*, 113-140.
- 852
- 853 42. Frydrychová, R., Grossmann, P., Trubac, P., Vítková, M., & Marec, F.E. Phylogenetic distribution
854 of TTAGG telomeric repeats in insects. *Genome* **2004**, *47*, 163-178. 10.1139/g03-100
- 855 43. Schön, I, Martens, K. No slave to sex. *Proc. R. Soc. Lond. B* **2003**, *270*, 827-833.
856 <https://doi.org/10.1098/rspb.2002.2314>
- 857 44. Altschul, S.F., Gish, W., Miller, W., Myers, E.W. & Lipman, D.J. Basic local alignment search tool.
858 *J. Mol. Biol.*, **1990**, *215*, 403-410. 10.1016/S0022-2836(05)80360-2
- 859 45. Tran Van, P., Anselmetti, Y., Bast, J., Dumas, Z., Galtier, N., Jaron, K., Martens, K., Parker, D.,
860 Robinson-Rechavi, M., Schwander, T., Simion, P. & Schön, I. First annotated genomes of draft
861 genomes of three non-marine ostracods (Ostracoda, Crustacea) with different reproductive
862 modes. *G3, accepted*.
863 bioRxiv 2020.12.02.409169; doi: <https://doi.org/10.1101/2020.12.02.409169>
- 864 46. Flutre, T., Duprat, E., Feuillet, C., Quesneville, H. Considering transposable element
865 diversification in *de novo* annotation approaches. *PLoS One*, **2011**, *6*, e16526. doi:
866 10.1371/journal.pone.0016526
- 867 47. Quesneville, H., Bergman, C.M., Andrieu, O., Autard, D., Nouaud, D., Ashburner, M.,
868 Anxolabehere, D. Combined evidence annotation of transposable elements in genome
869 sequences. *PLoS Computat. Biol.*, **2005**, *1*, 166-175. doi:10.1371/journal.pcbi.0010022
- 870 48. Wicker, T., Sabot, F., Hua-Van, A., Bennetzen, J.L., Capy, P., Chalhoub, B., Flavell, A., Leroy, P.,
871 Morgante, M., Panaud, O., et al. A unified classification system for eukaryotic transposable
872 elements. *Nat. Rev. Genet.*, **2007**, *8*, 973-982. <https://doi.org/10.1038/nrg2165>
- 873 49. Smit, A.F.A., Hubley, R., Green, P. RepeatMasker Open-4.0. 2013-2015. Available online:
874 <http://www.repeatmasker.org>.
- 875 50. Stanke, M., Schöffmann, O., Morgenstern, B., Waack, S. Gene prediction in eukaryotes with a
876 generalized hidden Markov model that uses hints from external sources. *BMC Bioinform.*, **2006**, *7*,
877 62. <https://doi.org/10.1186/1471-2105-7-62>
- 878 51. Quinlan, A.R., Hall, I.M. BEDTools: a flexible suite of utilities for comparing genomic features.
879 *Bioinformatics*, **2010**, *26*, 841-842. doi:10.1093/bioinformatics/btq033
- 880 52. Wickham, H. *ggplot2: Elegant Graphics for Data Analysis*. 2016. Springer-Verlag New York.
- 881 53. R Core Team. R: A language and environment for statistical computing. 2013. R Foundation for
882 Statistical Computing, Vienna, Austria. <http://www.R-project.org/>. Author 1, A.B. (University,
883 City, State, Country); Author 2, C. (Institute, City, State, Country). Personal communication,
884 2012.
- 885 54. Krzywinski, M., Schein, J., Birol, I., Connors, J., Gascoyne, R., Horsman, D., Jones, S.J., Marra,
886 M.A. Circos: an information aesthetic for comparative genomics. *Genome Res.*, **2009**, *19*, 1639-
887 1645. 10.1101/gr.092759.109
- 888 55. Waterhouse, R.M., Seppey, M., Simão, F.A., Manni, M., Ioannidis, P., Klioutchnikov, G.,
889 Kriventseva, E.V., Zdobnov, E.M. BUSCO Applications from Quality Assessments to Gene
890 Prediction and Phylogenomics, *Mol. Biol. Evol.*, **2018**, *35*, 543-548.
891 <https://doi.org/10.1093/molbev/msx319>
- 892 56. Simão, F.A., Waterhouse, R.M., Ioannidis, P., Kriventseva, E.V., Zdobnov, E.M. BUSCO:
893 assessing genome assembly and annotation completeness with single-copy orthologs.
894 *Bioinformatics*, **2015**, *31*, 3210-3212. <https://doi.org/10.1093/bioinformatics/btv351>
- 895 57. Edgar RC: MUSCLE: a multiple sequence alignment method with reduced time and space
896 complexity. *BMC Bioinformatics* 2004, *5*:113.
- 897 58. Zimmermann, L., Stephens, A., Nam, S.Z., Rau, D., Kubler, J., Lozajic, M., Gabler, F., Soding, J.,
898 Lupas, A.N., Alva, V. A completely reimplemented MPI bioinformatics toolkit with a new
899 HHpred server at its core. *J. Mol. Biol.*, **2018**, *430*, 2237-2243. 10.1016/j.jmb.2017.12.007
- 900 59. Waterhouse, A.M., Procter, J.B., Martin, D.M.A., Clamp, M., Barton, G.J. Jalview Version 2—a
901 multiple sequence alignment editor and analysis workbench. *Bioinformatics*, **2009**, *25*, 1189-1191.
902 10.1093/bioinformatics/btp033

Deleted: ¶

Formatted: Font: 10 pt, English (US)

Formatted: Left, Indent: Left: 0 cm, Hanging: 0,75 cm

Formatted: Font: 10 pt, English (US)

Formatted: Font: 10 pt, Italic

Formatted: Font: 10 pt

Formatted: Font: 10 pt

- 904 60. Burke, W.D., Malik, H.S., Jones, J.P., Eickbush, T.H. The domain structure and retrotransposition
905 mechanism of R2 elements are conserved throughout arthropods. *Mol. Biol. Evol.*, **1999**, *16*, 502-
906 511. [10.1093/oxfordjournals.molbev.a026132](https://doi.org/10.1093/oxfordjournals.molbev.a026132)
- 907 61. Volf, J.N., Körting, C., Froschauer, A., Sweeney, K., Scharl, M. Non-LTR retrotransposons
908 encoding a restriction enzyme-like endonuclease in vertebrates. *J. Mol. Evol.*, **2001**, *52*, 351-360.
909 [10.1007/s002390010165](https://doi.org/10.1007/s002390010165)
- 910 62. Biedler, J.K., Chen, X., Tu, Z. Horizontal transmission of an R4 clade non-long terminal repeat
911 retrotransposon between the divergent *Aedes* and *Anopheles* mosquito genera. *Insect Mol. Biol.*,
912 **2015**, *24*, 331-337. [10.1111/imb.12160](https://doi.org/10.1111/imb.12160)
- 913 63. Shivram, H., Cawley, D., Christensen, S.M. Targeting novel sites: The N-terminal DNA binding
914 domain of non-LTR retrotransposons is an adaptable module that is implicated in changing site
915 specificities. *Mob. Genet. Elements*, **2011**, *1*, 169-178. [10.4161/mge.1.3.18453](https://doi.org/10.4161/mge.1.3.18453)
- 916 64. Kojima, K.K., Fujiwara, H. Cross-genome screening of novel sequence-specific non-LTR
917 retrotransposons: various multicopy RNA genes and microsatellites are selected as targets. *Mol.*
918 *Biol. Evol.*, **2004**, *21*, 207-217. [10.1093/molbev/msg235](https://doi.org/10.1093/molbev/msg235)
- 919 65. Deng, Y., Liu, J., Zheng, Q., Yong, W., Lu, M. Structures and polymorphic interactions of two
920 heptad-repeat regions of the SARS virus S2 protein. *Structure*, **2006**, *14*, 889-899.
921 [10.1016/j.str.2006.03.007](https://doi.org/10.1016/j.str.2006.03.007)
- 922 66. Cai, Y., Zhang, J., Xiao, T., Peng, H., Sterling, S.M., Walsh, R.M., Jr., Rawson, S., Rits-Volloch, S.,
923 Chen, B. Distinct conformational states of SARS-CoV-2 spike protein. *Science*, **2020**, *369*, 1586-
924 1592. [10.1126/science.abd4251](https://doi.org/10.1126/science.abd4251)
- 925 67. Dietrich, M.H., Ogden, K.M., Long, J.M., Ebenhoch, R., Thor, A., Dermody, T.S., Stehle, T.
926 Structural and functional features of the reovirus σ 1 tail. *J. Virol.*, **2018**, *92*, 14. [10.1128/JVI.00336-
927 18](https://doi.org/10.1128/JVI.00336-18)
- 928 68. Malik, H.S., Henikoff, S., Eickbush, T.H. Poised for contagion: evolutionary origins of the
929 infectious abilities of invertebrate retroviruses. *Genome Res.*, **2000**, *10*, 1307-1318.
930 [10.1101/gr.145000](https://doi.org/10.1101/gr.145000)
- 931 69. Rodriguez, F., Kenefick, A.W., Arkhipova, I.R. LTR-retrotransposons from bdelloid rotifers
932 capture additional ORFs shared between highly diverse retroelement types. *Viruses*, **2017**, *9*, 78.
933 [10.3390/v9040078](https://doi.org/10.3390/v9040078)
- 934 70. Colbourne, J.K., Pfrender, M.E., Gilbert, D., Thomas, W.K., Tucker, A., Oakley, T.H., Tokishita,
935 S., Aerts, A., Arnold, G.J., Basu, M.K., et al. The ecoresponsive genome of *Daphnia pulex*. *Science*,
936 **2011**, *331*, 555-561. [10.1126/science.1197761](https://doi.org/10.1126/science.1197761)
- 937 71. Ye, Z., Xu, S., Spitze, K., Asselman, J., Jiang, X., Ackerman, M.S., Lopez, J., Harker, B., Raborn,
938 R.T., Thomas, W.K., Ramsdell, J. A new reference genome assembly for the microcrustacean
939 *Daphnia pulex*. G3: Genes, Genomes, Genetics, **2017**, *7*, 1405-1416.
940 <https://doi.org/10.1534/g3.116.038638>
- 941 72. Blanc-Mathieu, R., Perfus-Barbeoch, L., Aury, J.M., Da Rocha, M., Gouzy, J., Sallet, E., Martin-
942 Jimenez, C., Bailly-Bechet, M., Castagnone-Sereno, P., Flot, J.F. et al. Hybridization and
943 polyploidy enable genomic plasticity without sex in the most devastating plant-parasitic
944 nematodes. *PLoS Genet.*, **2017**, *13*, e1006777. <https://doi.org/10.1371/journal.pgen.1006777>
- 945 73. Schaack, S., Gilbert, C., Feschotte, C. Promiscuous DNA: horizontal transfer of transposable
946 elements and why it matters for eukaryotic evolution. *Trends Ecol. Evol.*, **2010**, *25*, 537-546.
947 [doi:10.1016/j.tree.2010.06.001](https://doi.org/10.1016/j.tree.2010.06.001)
- 948 74. Dupeyron, M., Leclercq, S., Cerveau, N., Bouchon, D., Gilbert, C. Horizontal transfer of
949 transposons between and within crustaceans and insects. *Mobile DNA*, **2014**, *5*, 4.
950 [doi:10.1186/1759-8753-5-4](https://doi.org/10.1186/1759-8753-5-4)
- 951 75. Wallau, G.L., Vieira, C., Loreto, É. Genetic exchange in eukaryotes through horizontal transfer:
952 connected by the mobilome. *Mobile DNA*, **2018**, *9*, 6. [doi:10.1186/s13100-018-0112-9](https://doi.org/10.1186/s13100-018-0112-9)
- 953 76. Metzger, M.J., Paynter, A.N., Siddall, M.E., Goff, S.P. Horizontal transfer of retrotransposons
954 between bivalves and other aquatic species of multiple phyla. *Proc. Natl. Acad. Sci. U.S.A.*, **2018**,
955 *115*, E4227-E4235. [doi:10.1073/pnas.1717227115](https://doi.org/10.1073/pnas.1717227115)

- 956 77. Arkhipova, I.R., Rodriguez, F. Genetic and epigenetic changes involving (retro)transposons in
957 animal hybrids and polyploids. *Cytogenet. Genome Res.*, **2013**, *140*, 295-311.
958 <https://doi.org/10.1159/000352069>
- 959 78. Huang, C.R., Burns, K.H., Boeke, J.D. Active transposition in genomes. *Ann. Rev. Gen.*, **2012**, *46*,
960 651-675. doi:10.1146/annurev-genet-110711-155616
- 961 79. Arkhipova, I.R. Neutral theory, transposable elements, and eukaryotic genome evolution. *Mol.*
962 *Biol. Evol.*, **2018**, *35*, 332-1337. doi: 10.1093/molbev/msy083
- 963 80. Petersen, M., Armisén, D., Gibbs, R.A., Hering, L., Khila, A., Mayer, G., Richards, S., Niehuis, O.,
964 Misof, B. Diversity and evolution of the transposable element repertoire in arthropods with
965 particular reference to insects. *BMC Evol. Biol.*, **2019**, *19*, 11. doi: 10.1186/s12862-018-1324-9
- 966 81. Song, L., Bian, C., Luo, Y., Bian, C., Luo, Y., Wang, L., You, X., Li, J., *et al.* Draft genome of the
967 Chinese mitten crab, *Eriocheir sinensis*. *GigaSci*, **2016**, *5*, 5. doi:10.1186/s13742-016-0112-y
- 968 82. Yuan, J., Gao, Y., Zhang, X., Wei, J., Liu, C., Li, F., Xiang, J. Genome sequences of marine shrimp
969 *Exopalaemon carinicauda* Holthuis provide insights into genome size evolution of Caridea. *Marine*
970 *drugs*, **2017**, *15*, 213. doi:10.3390/md15070213
- 971 83. Kao, D., Lai, A.G., Stamatakis, E., Rosic, S., Konstantinides, N., Jarvis, E., Di Donfrancesco, A.,
972 Pouchkina-Stancheva, N., Semon, M., Grillo, M., Bruce, H. The genome of the crustacean
973 *Parhyale hawaiiensis*, a model for animal development, regeneration, immunity and lignocellulose
974 digestion. *Elife*, **2016**, *5*, e20062. 10.7554/eLife.20062
- 975 84. Muszewska, A., Steczkiewicz, K., Stepniewska-Dziubinska, M. *et al.* Transposable elements
976 contribute to fungal genes and impact fungal lifestyle. *Sci. Rep.*, **2019**, *9*, 4307. doi:10.1038/s41598-
977 019-40965-0
- 978 85. Hartley, G., O'Neill, R.J. Centromere repeats: hidden gems of the genome. *Genes*, **2019**, *10*, 223.
979 doi:10.3390/genes10030223
- 980 86. Gao, D., Jiang, N., Wing, R.A., Jiang, J., Jackson, S.A. Transposons play an important role in the
981 evolution and diversification of centromeres among closely related species. *Front. Plant*
982 *Sci.*, **2015**, *6*, 216. doi:10.3389/fpls.2015.00216
- 983 87. Pardue, M.-L., DeBaryshe, P.G. Retrotransposons that maintain chromosome ends. *Proc. Natl.*
984 *Acad. Sci. U.S.A.*, **2011**, *108*, 20317-20324. <https://doi.org/10.1073/pnas.1100278108>
- 985 88. Gladyshev, E.A., Arkhipova, I.R. Telomere-associated endonuclease-deficient Penelope-like
986 retroelements in diverse eukaryotes. *Proc. Natl. Acad. Sci. U.S.A.*, **2007**, *104*, 9352-9357.
987 <https://doi.org/10.1073/pnas.0702741104>
- 988 89. Goodier, J.L. Restricting retrotransposons: a review. *Mobile DNA*, **2016**, *7*, 16. doi:10.1186/s13100-
989 016-0070-z
- 990 90. Rodriguez, F., Arkhipova, I.R. Multitasking of the piRNA silencing machinery: targeting
991 transposable elements and foreign genes in the bdelloid rotifer *Adineta vaga*. *Genetics*, **2016**, *203*,
992 255-268. doi: 10.1534/genetics.116.186734
- 993 91. Rodriguez, F., Arkhipova, I.R. Multitasking of the piRNA silencing machinery: targeting
994 transposable elements and foreign genes in the bdelloid rotifer *Adineta vaga*. *Genetics*, **2016**, *203*,
995 255-268. doi: 10.1534/genetics.116.186734
- 996 92. Molaro, A., Malik, H.S. Hide and seek: how chromatin-based pathways silence retroelements in
997 the mammalian germline. *Curr. Opin. Genet. Dev.*, **2016**, *37*, 51-58.
998 doi: 10.1016/j.gde.2015.12.001
- 999 93. Schön, I., Kamiya, T., Van den Berghe, T., Van den Broecke, L., Martens, K. The evolutionary
1000 history of novel *Cardinium* strains and their non-marine ostracod (Crustacea) hosts. *Mol. Phyl.*
1001 *Evol.*, **2019**, *130*, 406-415. 10.1016/j.ympev.2018.09.008
- 1002 94. Martens, K., Horne, D.J., Griffiths, H.I. Age and diversity of non-marine ostracods. In: *Sex and*
1003 *Parthenogenesis. Evolutionary Ecology of Reproductive Modes in Non-Marine Ostracods*; Martens, K.,
1004 Ed.; Backhuys Publishers, Leiden, 1998, pp. 37-55.
- 1005 95. Wolfe, J.M., Daley, A.C., Legg, D.A., Edgcombe, G.D. Fossil calibrations for the arthropod Tree
1006 of Life. *Earth-Sci. Rev.*, **2016**, *160*, 43-110. <https://doi.org/10.1016/j.earscirev.2016.06.008>

1007 **Publisher’s Note:** MDPI stays neutral with regard to jurisdictional claims in published maps and institutional
1008 affiliations.



© 2020 by the authors. Submitted for possible open access publication under the terms and conditions of the Creative Commons Attribution (CC BY) license (<http://creativecommons.org/licenses/by/4.0/>).

1009

